



Beam Steering using Space-Time Modulated Coding Metasurface Based on Reconfigurable Plasma Ionization

Mona Magdy Badawy¹, Anas Saber Zainud-Deen², Hend Abd El-Azem Malhat^{1,*}, Shaymaa Mostafa Gaber²

¹ Faculty of Electronic Engineering, Menofia University, Shibin el Kom, Menofia Governorate 6131567, Egypt

² Faculty of Engineering, Egyptian-Russian University (ERU), Cairo Governorate 11829, Egypt

ARTICLE INFO

Article history:

Received 10 October 2023

Received in revised form 19 December 2023

Accepted 12 February 2024

Available online 25 April 2024

Keywords:

Beam steering; Reconfigurable coding metasurface; Plasma; Time-switching sequences

ABSTRACT

This paper explores the use of space-time coding in beam steering, using 1-bit, 2-bit, and 3-bit reconfigurable coded meta-surfaces. By periodically changing the code arrangement in the time domain, a metasurface with code order in space and time is achieved. Selected codes are used to steer the beam in different directions for radar sensing systems applications. The phase of the harmonic signal is changed by controlling the position of different bits in each code sequence. The construction of 8×8 unit-cell elements (120×120×3.2 mm³) involves the use of a grounded dielectric container filled with inert-argon gas. The metasurface logic-state is controlled via the ionization degree of inert-gas with time-switching controlling the harmonic frequencies. Different time-switching sequences are investigated for beam steering. The proposed coding metasurface is analysed using CST Microwave Studio and the results are compared with the analytical solution using MATLAB.

1. Introduction

Recently, reconfigurable intelligent surfaces (RISs) are widely recognized as a promising technology for wireless 6G communication. The concept of digital meta-surfaces was put in 2014 [1-4]. Several reconfigurable antennas are employed to enable various functionalities that are used in the different applications [5,6]. Metasurface can configure the characteristics of EM-wave in microwave range. An RIS is a planar surface that consists of many elements, each of which can be reconfigurable and scattered [7-10]. The RIS gain is proportional to the square of the number of the unit-cell elements. In reconfigurable coding metasurface reconfigurable elements using diodes as active elements such as electronic switches, or using reconfigurable material such as plasma material or graphene are introduced. Field-programmable gate array (FPGA) is used to make programmable metasurface platform [2]. In space-coding, the code order is fixed with time, however, in space-time coding meta-surfaces is characterized by spatially and temporally variant properties. Digital

* Corresponding author.

E-mail address: er_honida1@yahoo.com

<https://doi.org/10.37934/araset.44.1.151159>

metasurface using the space-time coding is illustrated in [7,8]. The switching waveform affects the scattering patterns from RIS [9-12]. In time coding modulation, each switching order is a train of periodically repeating bits controlled via time-pulses applied to the control switch [2,13,14]. Plasma material has many advantages like stealth coupling off-on rapid switch mode, and repaid reconstruction [15-23]. Plasma reflectarray [17], transmitarray [18], frequency selective surfaces [19], and artificial magnetic conductors [20]. Reconfigurable time-modulated plasma arrays applied in beam-shaping and beam-steering were investigated in [11,24].

In this paper, the beam-steering is performed by controlling the different bits of each code. Comparisons between the full wave analysis using CST Microwave Studio and the analytical solution using MATLAB are investigated. The plasma construction has simple structure and low coupling. The plasma makes the structure to be reconfigurable with respect to its shape, working frequency and signal bandwidth on millisecond to microsecond timescales [25,26]. The radiation characteristics of the unit-cell are investigated. The time coding is used to feed an 8x8 elements. Beam scanning using 1-bit, 2-bit, and 3-bit is performed.

2. The Design of Coded Metasurface

In this section, the coding metasurface performance is evaluated both numerically and analytically. To verify the numerical results, isotropic elements are considered. MATLAB is used to calculate and plot the scattering pattern. The coding metasurface is constructed from $N \times N$ unit-cell elements with the same size in which each element is occupied by "0" or "1" element in 1-bit coding metasurfaces. The codes are extended to 2-bit and 3-bit cases. The reflection phases of 0° , 90° , 180° , and 270° degrees are used for 2-bit case and 0° , 45° , 90° , 135° , 180° , 225° , 270° , and 310° degrees are used for 3-bit case. The scattered pattern from the planar array illuminated by plane wave can be written as:

$$E(\theta, \varphi, t) = \text{unit cell pattern} \times \text{array factor} \quad (1)$$

$$= f(\theta, \varphi) \sum_{i=1}^{N^2} \Gamma_i(t) e^{j\beta\Psi}$$

where $\Psi = x_i u + y_i v$, $u = \sin\theta\cos\varphi$, $v = \sin\theta\sin\varphi$, (x_i, y_i) is the position of the i^{th} element. $f(\theta, \varphi)$ is the scattered pattern of the unit-cell at f_c , and $\beta = \frac{2\pi}{\lambda_c}$ is the wave-number. For the modulation period, T_o larger than T_c ($T_o \gg T_c$), the reflection coefficient can be expressed as

$$\Gamma_i(t) = \sum_{l=1}^L \Gamma_i^{(l)} U_{li}(t) \quad (2)$$

$\Gamma_i(t)$ is the time-modulated reflection coefficient and $U_{li}(t)$ is a periodic pulse function defined as:

$$U_{li}^{(l)}(t) = \begin{cases} 1 & (l-1)T_s \leq t \leq lT_s \\ 0 & \text{elsewhere} \end{cases} \quad (3)$$

Represents a rectangular pulse of width $T_s = T_o/L$ and $\Gamma_i^{(l)}$ denotes on one of the possible reflection-coefficient states (at the excitation frequency, f_c) of the coding element. For 1-bit case $\Gamma_i^{(l)} \in \{1, e^{j\pi}\}$ associated with the bits {0,1}, for a 2-bit case, $\Gamma_i^{(l)} \in \{1, e^{j\pi/2}, e^{j\pi}, e^{j3\pi/2}\}$, whereas for

a 3-bit $\Gamma_i^{(l)} \in \left\{1, e^{j\frac{\pi}{4}}, e^{j\frac{\pi}{2}}, e^{j\frac{3\pi}{4}}, e^{j\pi}, e^{j\frac{5\pi}{4}}, e^{j\frac{3\pi}{2}}, e^{j\frac{7\pi}{4}}\right\}$ case, Thus, the far-field scattering pattern of the coding metasurface at the m^{th} harmonic frequency is $f_c \pm mf_o$ given by,

$$E_m(\theta, \varphi) = f(\theta, \varphi) \sum_{i=1}^{N^2} a_m^i e^{j\beta\Psi} \quad (4)$$

$$a_m^i = \sum_{l=1}^L \frac{\Gamma_i^{(l)}}{L} \text{sinc}\left(\frac{m\pi}{L}\right) e^{-j\pi m(2l-1)} \quad (5)$$

Throughout the paper, $(f(\theta, \varphi) = 1)$ is assumed. By controlling the time-coding sequences of the individual elements, a set of complex reflection coefficients a_m^i are synthesized to control their scattering properties

3. Design of Plasma Metasurface Unit-Cell

The dispersive electrical properties of the plasma are modelled by Drude model given by [21],

$$\epsilon_r = 1 - \frac{f_p^2}{f_c(f_c - jf_v)} \quad (6)$$

where ϵ_r is the relative permittivity, f_c is the operating frequency, f_v is the collision frequency, and f_p is the plasma frequency which is related to the electron density n_e as

$$f_p = \frac{1}{2\pi} \sqrt{\frac{n_e e^2}{m_e \epsilon_0}} \quad (7)$$

where e and m_e are the electron charge and mass. The electron density of the ionized plasma medium is controlled by the applied DC voltage as given by [21]

$$V_B = \left(\frac{n_e \sqrt{eKT_e H_p^2}}{\epsilon_0} \right)^{2/3} \quad (8)$$

where K is Boltzmann constant, and T_e is the electron temperature. By increasing the plasma frequency, the electron density and then the plasma conductivity is increased at fixed operating frequency. It is found that plasma conductivity is affected by the electron density at a fixed collision frequency.

4. Results and Discussion

The dielectric cover of the unit cell has a thickness of H_c and a relative dielectric constant of $\epsilon_{rc}=3.4$ as shown in Figure 1. It is connected to a central cylinder with two arms of thickness t_c and placed on a dielectric grounded dielectric (FR4, $\epsilon_{rd}=4.6$, $\tan\delta=0.036$) with a thickness of H_s . The gas is ionized using DC voltage at a height of H_p . The reflection coefficient is calculated using the CST Microwave Studio, with the unit cell boundaries set to simulate an infinite array and consider mutual coupling between adjacent elements.

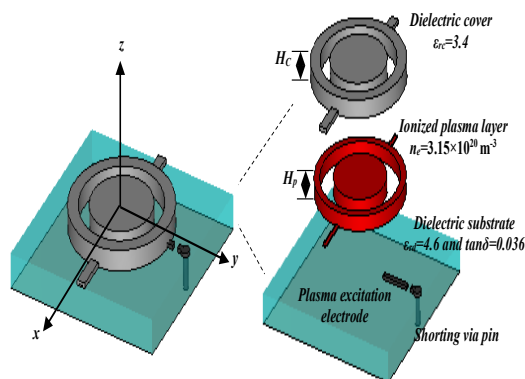


Fig. 1. Schematic of plasma unit-cell element

Figure 2(a) displays the phase variation of the reflection coefficient at 9 GHz with plasma frequency ranging from 4.5×10^{11} rad/sec to 16×10^{11} rad/sec, resulting in a phase variation of 0 to 309° degrees. Figure 2(b) shows the phase of the reflection coefficient of the unit cell element at different values of $\omega_{p1}=4.5 \times 10^{11}$ rad/sec, $\omega_{p2}=6.52 \times 10^{11}$ rad/sec, $\omega_{p3}=7.8 \times 10^{11}$ rad/sec, and $\omega_{p4}=10.8 \times 10^{11}$ rad/sec, with $\omega_{p1}=4.5 \times 10^{11}$ rad/sec representing bit “0” and $\omega_{p2}=10.8 \times 10^{11}$ rad/sec representing bit “1”.

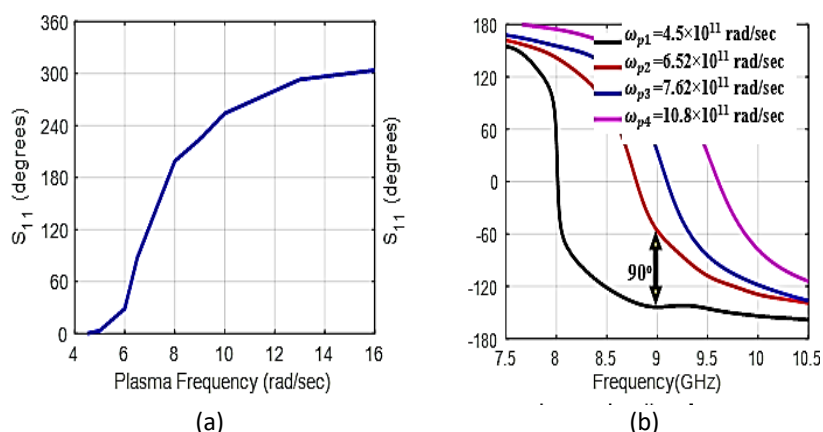


Fig. 2. Unit-cell performance characteristics

The dimensions of the unit-cell are illustrated in Table 1, while Table 2 lists the required plasma frequencies for 2-bit and 3-bit coding states of the unit cell element.

Table 1

The unit-cell dimensions (in millimetre)

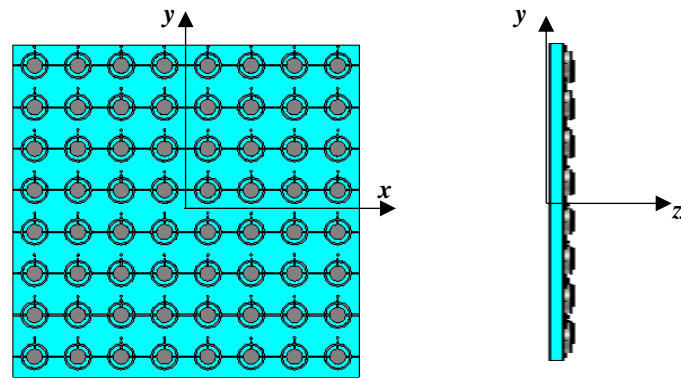
L_c	1.5	R_i	4.0	W_c	1.0
W	0.5	R_o	3.0	H_c	1.2
t_c	0.2	R_i	0.25	H_s	2.0
H_p	1.0	ϵ_{rc}	3.4	ϵ_{rd}	4.6

Table 2

The required plasma frequencies for 2-bit and 3-bit coding states of the unit cell

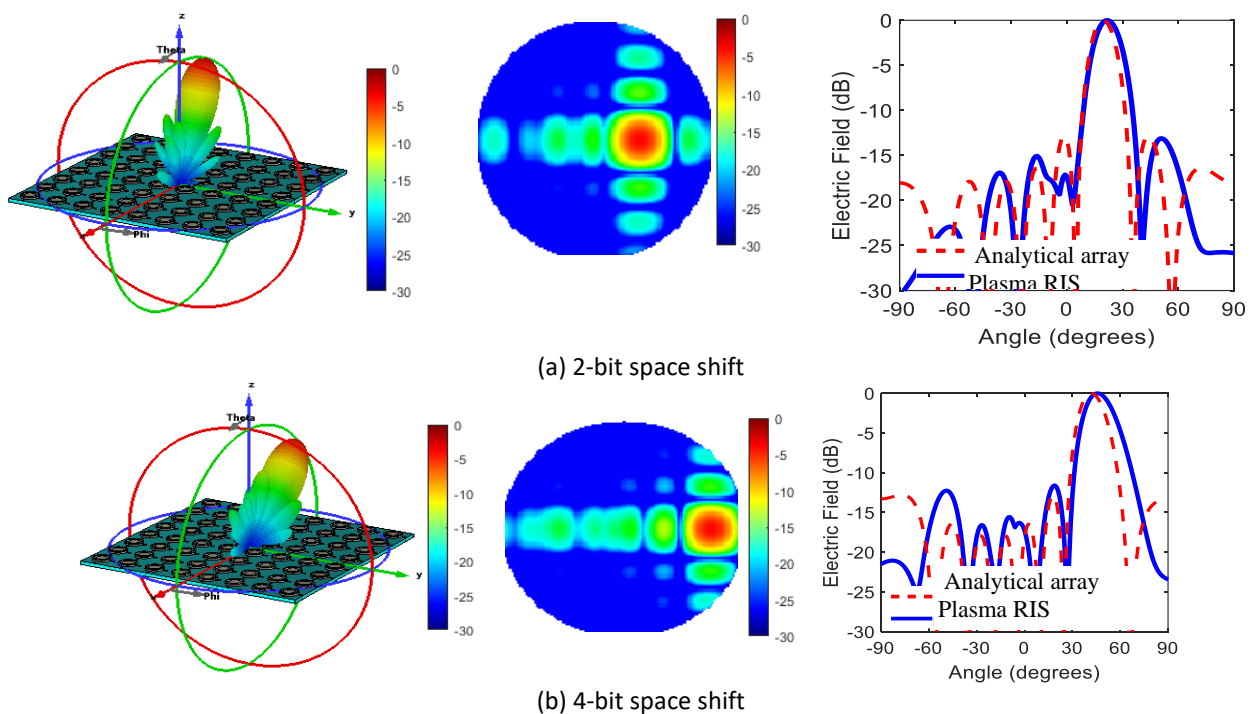
Coding Bits	Plasma Frequency (rad/sec)							
1-bit	4.5×10^{11}			7.62×10^{11}				
2-bit	4.5×10^{11}	6.52×10^{11}		7.62×10^{11}			10.8×10^{11}	
3-bit	4.5×10^{11}	6.19×10^{11}	6.52×10^{11}	6.98×10^{11}	7.62×10^{11}	9.03×10^{11}	10.8×10^{11}	16.82×10^{11}

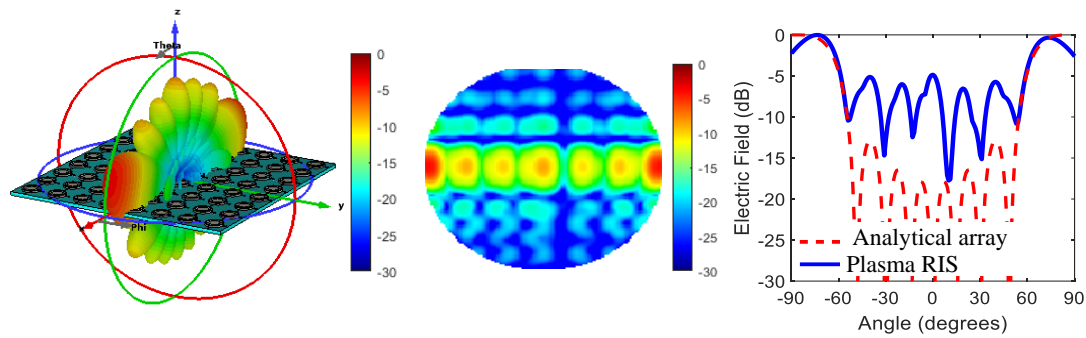
The proposed coding metasurface is depicted in Figure 3. The scattering patterns of the array, which is comprised of 8×8 ring plasma metamaterial elements, are simulated using CST Microwave Studio. The total size of the metasurface is $120 \times 120 \times 3.2$ mm³, with $L_c = \lambda_c / 2$. Each column has the same ionization voltage. For 1-bit, the reflection coefficient phase is either 0° or 180° degrees, for 2-bit it is 0° or 90° or 180° or 270° degrees, and for 3-bit it is 0° or 45° or 90° or 135° , 180° or 225° or 270° or 315° degrees.



(a) Top view (b) Side view
Fig. 3. The proposed coding metasurface

Figure 4 displays the scattered field for the 1-bit beam steering case. The sequence for the first time slot is 001000110111 ($L=12$), followed by 2-bit shifting for the next time slots, 4-bit shifting and six-bit shifting. The centre frequency is 9 GHz. The scattering patterns in the x - z plane at 9 GHz for each bit shift are compared with the analytical solution using Eq. (4). Due to the coupling between the elements, high sidelobe levels are obtained.

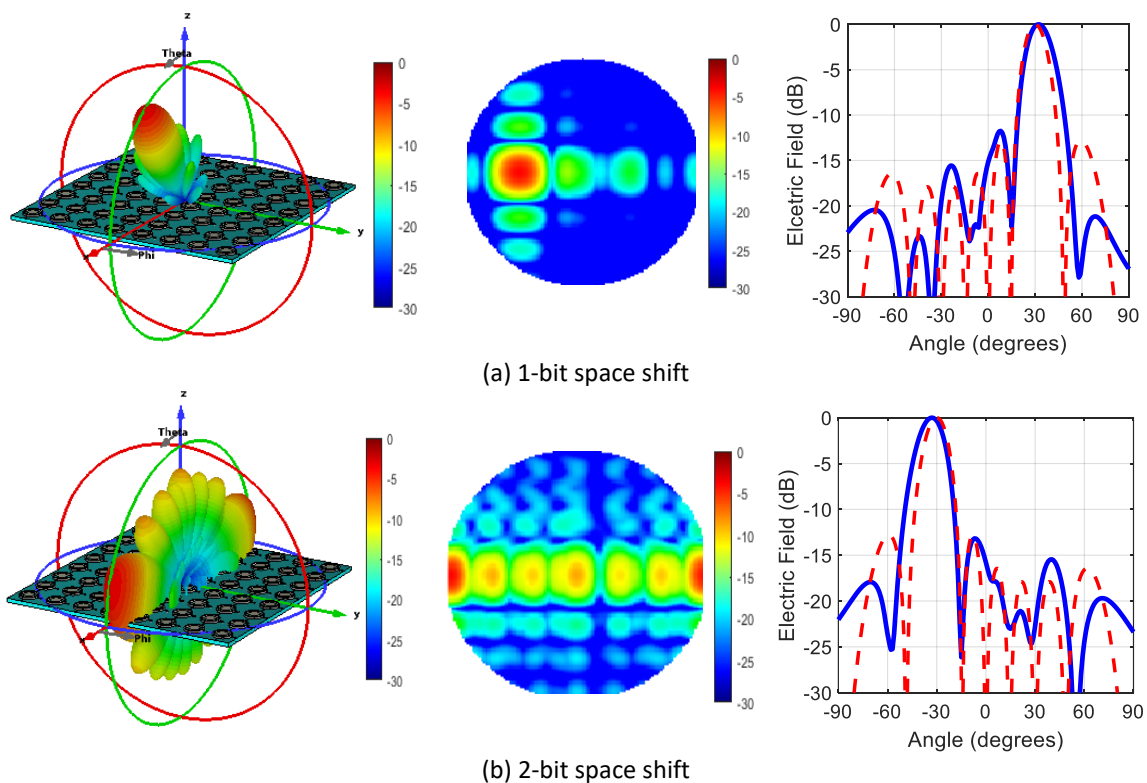




(c) 6-bit space shift

Fig. 4. The scattering patterns at 9 GHz for 1-bit coding case for different space shifts

The coding metasurface for 2-bit beam steering is made up of four coding elements, namely "00", "01", "10", and "11", each exhibiting a phase response of 0° , 90° , 180° , or 270° degrees, respectively. The number of time slots (L) is fixed at 4 for all elements in the array. Figure 5 shows the scattered patterns for the 1st harmonic frequency, with good agreement between the analytical and plasma RIS results. The scattering patterns for the subsequent time slots are also shown, with no-bit shifting, one-bit shifting, two-bit shifting, and three-bit shifting backward. The maximum direction of the beam varies depending on the harmonic frequency.



(a) 1-bit space shift

(b) 2-bit space shift

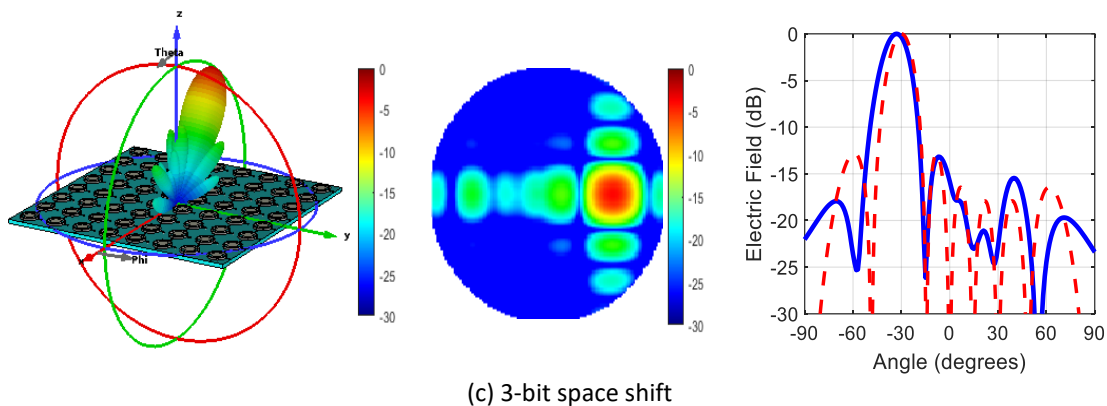


Fig. 5. The scattering patterns at 9 GHz for 2-bit coding case for different space shifts

In the case of 3-bit beam steering, the value of L is 8, which corresponds to the elements of the array (0, 1, 2, 3, 4, 5, 6, 7). Each element exhibits phase responses of 0° , 45° , 90° , 135° , 180° , 225° , 270° , or 315° degrees. The scattered patterns of the 1st harmonic component can be seen in Figure 6. The field patterns are shown for different bit shifting scenarios, 1-bit shifting, 3-bit shifting and 5-bit shifting.

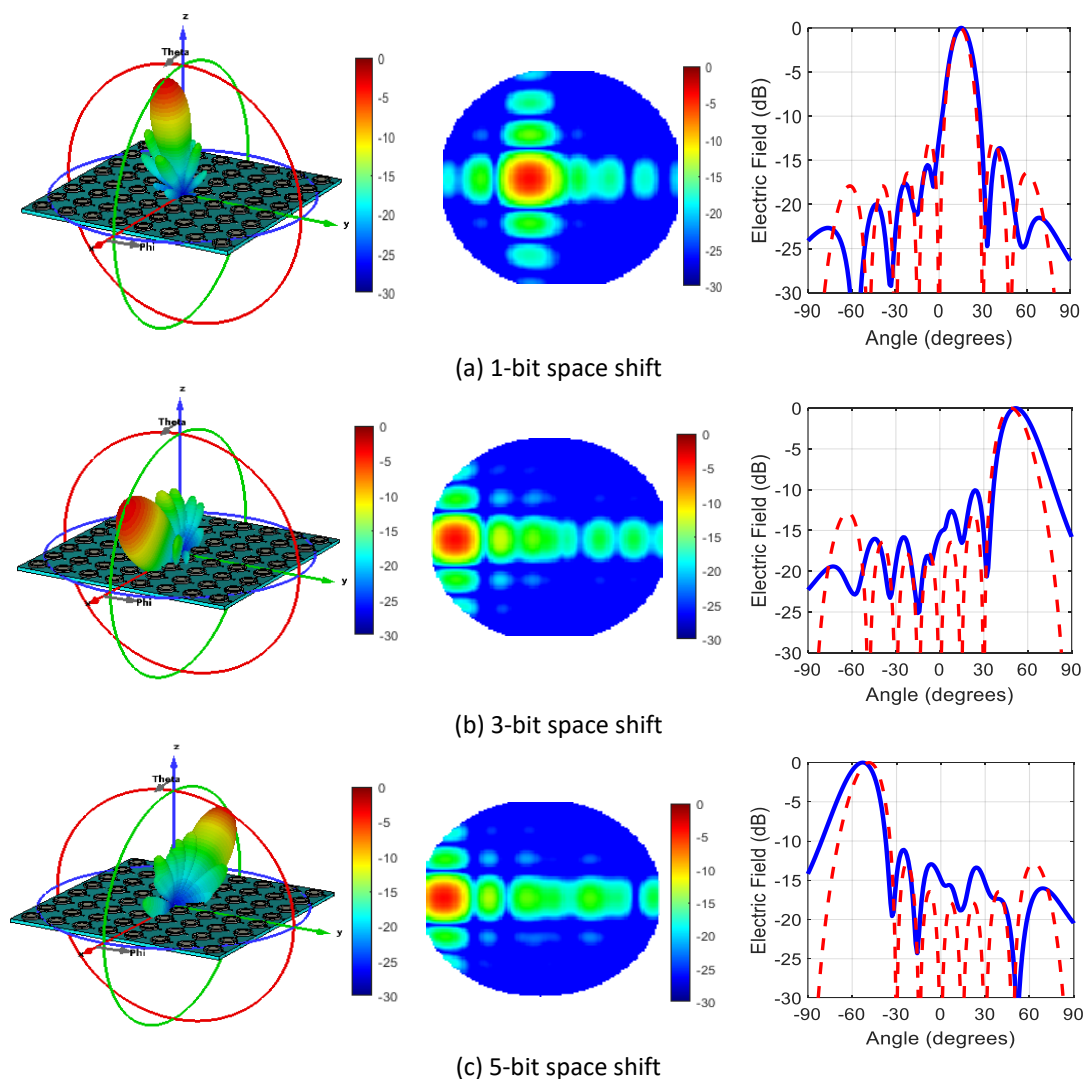


Fig. 6. The scattering patterns at 9 GHz for 3-bit coding case for different space shifts

4. Conclusion

The investigation focuses on the utilization of space-time coding metasurface for beam steering. The metasurface is composed of a 2-D array consisting of 8x8 elements with dimensions of 120x120x3.2 mm³. Each element is filled with gas, and the scattering from each unit cell is controlled using the plasma frequency. The radiation at harmonic frequencies is regulated through plasma ionization. Various time-switching sequences are examined to achieve beam steering. The results are obtained through both analytical solution and CST Microwave Studio simulator, and they exhibit good agreement. The space-time coding is demonstrated using different sequences, including 1-bit, 2-bit, and 3-bit reconfigurable coding metasurfaces. The scattered patterns are achieved by employing plasma ionization. The beam steering of the coding metasurface is showcased by electronically shifting the bits of the selected code. Additionally, a faster switching scheme utilizing plasma ionization gas is explored for phase modulation, which can be employed to steer the beam of the structure. This technique holds potential applications in radar sensing and multipoint communications.

Acknowledgement

This research was not funded by any grant.

References

- [1] Della Giovampaola, Cristian, and Nader Engheta. "Digital metamaterials." *Nature materials* 13, no. 12 (2014): 1115-1121. <https://doi.org/10.1038/nmat4082>
- [2] Cui, Tie Jun, Mei Qing Qi, Xiang Wan, Jie Zhao, and Qiang Cheng. "Coding metamaterials, digital metamaterials and programmable metamaterials." *Light: science & applications* 3, no. 10 (2014): e218-e218. <https://doi.org/10.1038/lssa.2014.99>
- [3] Moosa, Salmah, Anis Nadia Mohd Faisal Mahadeven, Kamyar Shameli, and Sin-Yeang Teow. "Physiochemical synthesis of Silver/Kaolinite nanocomposites and study their antibacterial properties." *Journal of Research in Nanoscience and Nanotechnology* 1, no. 1 (2021): 1-11. <https://doi.org/10.37934/jrnn.1.1.111>
- [4] Wang, Dan, Terh Jing Khoo, and Zhangfei Kan. "Exploring the application of digital data management approach for facility management in Shanghai's high-rise buildings." *Progress in Energy and Environment* (2020): 1-15.
- [5] Zurghiba, Hizanorhuda, Kumaran Kadirgama, Norazlianie Sazali, Muhamad Mat Noor, Rosli Abu Bakar, Sivarao Subramonian, Talal Yusaf *et al.*, "Enhancing Heat Transfer in Compact Automotive Engines using Hybrid Nano Coolants." *Journal of Advanced Research in Applied Sciences and Engineering Technology* 32, no. 2 (2023): 314-326. <https://doi.org/10.37934/araset.32.2.314326>
- [6] Tran, Nguyen Minh, Muhammad Miftahul Amri, Je Hyeon Park, Dong In Kim, and Kae Won Choi. "Reconfigurable-intelligent-surface-aided wireless power transfer systems: analysis and implementation." *IEEE Internet of Things Journal* 9, no. 21 (2022): 21338-21356. <https://doi.org/10.1109/JIOT.2022.3179691>
- [7] Zhang, Lei, Xiao Qing Chen, Shuo Liu, Qian Zhang, Jie Zhao, Jun Yan Dai, Guo Dong Bai *et al.*, "Space-time-coding digital metasurfaces." *Nature communications* 9, no. 1 (2018): 4334. <https://doi.org/10.1038/s41467-018-06802-0>
- [8] Zhang, Lei, Jun Yan Dai, Massimo Moccia, Giuseppe Castaldi, Tie Jun Cui, and Vincenzo Galdi. "Recent advances and perspectives on space-time coding digital metasurfaces." *EPJ Applied Metamaterials* 7 (2020): 7. <https://doi.org/10.1051/epjam/2020007>
- [9] Bang, Sanghun, Jeonghyun Kim, Gwanho Yoon, Takuo Tanaka, and Junsuk Rho. "Recent advances in tunable and reconfigurable metamaterials." *Micromachines* 9, no. 11 (2018): 560. <https://doi.org/10.3390/mi9110560>
- [10] Tran, Nguyen Minh, Muhammad Miftahul Amri, Je Hyeon Park, Dong In Kim, and Kae Won Choi. "Reconfigurable-intelligent-surface-aided wireless power transfer systems: analysis and implementation." *IEEE Internet of Things Journal* 9, no. 21 (2022): 21338-21356. <https://doi.org/10.1109/JIOT.2022.3179691>
- [11] Bao, Lei, and Tie Jun Cui. "Tunable, reconfigurable, and programmable metamaterials." *Microwave and Optical Technology Letters* 62, no. 1 (2020): 9-32. <https://doi.org/10.1002/mop.32164>
- [12] Wang, Di, Li-Zheng Yin, Tie-Jun Huang, Feng-Yuan Han, Zi-Wen Zhang, Yun-Hua Tan, and Pu-Kun Liu. "Design of a 1 bit broadband space-time-coding digital metasurface element." *IEEE Antennas and Wireless Propagation Letters* 19, no. 4 (2020): 611-615. <https://doi.org/10.1109/LAWP.2020.2973424>

- [13] Gholami, Mehdi, Ehsan Sadeghi, and Mohammad Neshat. "A New Look at the Coding in Time-Modulated Arrays." *International Journal of Information and Communication Technology Research* 13, no. 4 (2021): 1-7. <https://doi.org/10.52547/itrc.13.4.1>
- [14] Vosoughitabar, Shaghayegh, and Chung-Tse Michael Wu. "Programming nonreciprocity and harmonic beam steering via a digitally space-time-coded metamaterial antenna." *Scientific reports* 13, no. 1 (2023): 7338. <https://doi.org/10.1038/s41598-023-34195-8>
- [15] Kumar, Rajneesh, and Dhiraj Bora. "A reconfigurable plasma antenna." *Journal of Applied Physics* 107, no. 5 (2010). <https://doi.org/10.1063/1.3318495>
- [16] Badawy, Mona M., Hend Abd El-Azem Malhat, Saber Helmy Zainud-Deen, and Kamal Hassan Awadalla. "A simple equivalent circuit model for plasma dipole antenna." *IEEE Transactions on Plasma Science* 43, no. 12 (2015): 4092-4098. <https://doi.org/10.1109/TPS.2015.2494626>
- [17] Malhat, Hend Abd El-Azem, Mona M. Badawy, Saber Helmy Zainud-Deen, and Kamal H. Awadalla. "Dual-mode plasma reflectarray/transmitarray antennas." *IEEE Transactions on Plasma Science* 43, no. 10 (2015): 3582-3589. <https://doi.org/10.1109/TPS.2015.2440237>
- [18] Zainud-Deen, S. H., Hend A. Malhat, S. M. Gaber, and K. H. Awadalla. "Beam steering plasma reflectarray/transmitarray antennas." *Plasmonics* 9 (2014): 477-483. <https://doi.org/10.1007/s11468-013-9645-4>
- [19] Zainud-Deen, Saber Helmy, Hend Abd El-Azem Malhat, and Nagwa Adel Shabayek. "Reconfigurable RCS reduction from curved structures using plasma based FSS." *Plasmonics* 15, no. 2 (2020): 341-350. <https://doi.org/10.1007/s11468-019-01048-y>
- [20] Malhat, Hend Abd El-Azem, and Saber Helmy Zainud-Deen. "Plasma-based artificial magnetic conductor for polarization reconfigurable dielectric resonator antenna." *Plasmonics* 15, no. 6 (2020): 1913-1924. <https://doi.org/10.1007/s11468-020-01189-5>
- [21] Malhat, Hend Abd El-Azem, and Anas Saber Zainud-Deen. "Dual/circular polarization beam shaping of time-modulated plasma-based magneto-electric dipole antenna arrays." *Optical and Quantum Electronics* 54, no. 2 (2022): 111. <https://doi.org/10.1007/s11082-021-03482-x>
- [22] Berahim, Muhammad Syahizul Aidi, Mohd Fadhil Majnis, and Mustaffa Ali Azhar Taib. "Formation of titanium dioxide nanoparticles by anodization of valve metals." *Progress in Energy and Environment* (2018): 11-19.
- [23] Samat, Nazrul Azlan Abdul, Norfifah Bachok, and Norihan Md Arifin. "Carbon Nanotubes (CNTs) Nanofluids Flow and Heat Transfer under MHD Effect over a Moving Surface." *Journal of Advanced Research in Micro and Nano Engineering* 9, no. 1 (2022): 1-8. <https://doi.org/10.37934/arfmts.103.1.165178>
- [24] Malhat, Hend Abd El-Azem, and Anas Saber Zainud-Deen. "Beam-shaping technique for plasma magneto-electric dipole planar array based on time-modulation and particle swarm optimization." *Wireless Networks* 28, no. 7 (2022): 3001-3018. <https://doi.org/10.1007/s11276-022-03001-0>
- [25] Kumar, Rajneesh, and Dhiraj Bora. "Experimental study of parameters of a plasma antenna." *Plasma Science and Technology* 12, no. 5 (2010): 592. <https://doi.org/10.1088/1009-0630/12/5/17>
- [26] Zhao, Jiansen, Zhen Sun, Yuxiang Ren, Lu Song, Shengzheng Wang, Wei Liu, Zhe Yu, and Yuhan Wei. "Experimental characteristics of 2.45 GHz microwave reconfigurable plasma antennas." *Journal of Physics D: Applied Physics* 52, no. 29 (2019): 295202. <https://doi.org/10.1088/1361-6463/ab1b0a>